Lung anti-oxidant depletion: a predictive indicator of cellular stress induced by ambient fine particles

Belinda CROBEDDU[1], Isabelle BAUDRIMONT[2], Juliette DEWEIRDT[2], Jean SCIARE[3,4], Anne BADEL[1,5], Anne Claude CAMPROUX[1,5], Linh Chi BUI[1], Armelle BAEZA SQUIBAN[1]*

[1]: Université de Paris, BFA, UMR 8251 CNRS, F-75013, Paris, France.

[2]: Université de Bordeaux, Centre de Recherche Cardio-Thoracique de Bordeaux U1045, F-33604, Pessac, France

[3]: Laboratoire des Sciences du Climat et de l'Environnement, CEA-CNRS-UVSQ, F-91190 Gif sur Yvette, France

[4] : Energy, Environment and Water Research Center, The Cyprus Institute, 2121, Aglantzia, Cyprus

[5]: Université de Paris, BFA, UMR 8251, CNRS, ERL 1133, Inserm, F-75013 Paris, France

*: Corresponding author – Armelle BAEZA-SQUIBAN, Univ de Paris, Unit of Functional and Adaptive Biology (BFA) UMR 8251 CNRS, 5 rue Thomas Mann, F-75013, Paris, France – +33 1 57 27 83 35 – baeza@univ-paris-diderot.fr

Running title: oxidative potential of $PM_{2.5}$.

Abbreviations: OP: oxidative potential, PM2.5: particulate matter with an aerodynamic diameter < 2.5 µm; NCI-H292: human bronchial epithelial cell line; IL-8: interleukin 8; PAH: polycyclic aromatic hydrocarbons, HPAEC, human pulmonary artery endothelial cells, Traf: Traffic, BB: biomass burning, AA: ascorbic acid, GSH: glutathione.

1

Abstract

Regulations on ambient particulate matter (PM) are becoming more stringent due to adverse health effects arising from PM exposure. PM-induced oxidant production is a key mechanism behind the observed health effects and is heavily dependent on PM composition. Measurement of the intrinsic oxidative potential (OP) of PM could provide an integrated indicator of PM bioreactivity, and could serve as a better metric of PM hazard exposure than PM mass concentration. The OP of two chemically-contrasted $PM_{2.5}$ samples was compared through four acellular assays and OP predictive capability was evaluated in different cellular assays on two *in vitro* lung cell models. $PM_{2.5}$ collected in Paris at site close to the traffic exhibited a systematically higher OP in all assays compared to $PM_{2.5}$ enriched in particles from domestic wood burning. Similar results were obtained for oxidative stress, expression of anti-oxidant enzymes and pro-inflammatory chemokine in human bronchial epithelial and endothelial cells. The strongest correlations between OP assays and cellular responses were observed with the antioxidant (ascorbic acid and glutathione) depletion (OP^{AO}) assay. Multivariate regression analysis from OP daily measurements suggested that OP^{AO} was strongly correlated with PAH at traffic site while it was correlated with potassium for the domestic wood burning sample.

Keywords: $PM_{2.5}$, lung, oxidative potential, oxidative stress, traffic, biomass burning

Introduction

Three decades of extensive epidemiological and experimental investigations have demonstrated the impact of air quality on health and the key role played by fine airborne particles[1]. These $PM_{2.5}$ (Particulate Matter with an aerodynamic diameter below 2.5µm), due to their small size and chemical composition, have been associated with a range of health effects both within the respiratory tract and in a broader systemic context[2].

While policies have been implemented to reduce exposure to PM, the efficiency of these policies is hindered by a lack of knowledge regarding the involvement of individual particle components in specific health effects. Indeed, the World Health Organization, in the "Review of evidence on health aspects of air pollution" published in 2013, underlines that several components contribute to the health effects induced by $PM_{2.5}$, but indications are still insufficient to differentiate individual chemical components (or sources) that are more strictly related to specific health outcomes[3]. Actually, regulation of particles is typically based on PM mass measurement and does not take into account the chemical composition that drives particle toxicity. Particle composition can significantly change as a function of location and period of the year, with some components exhibiting low toxicity such as inorganic ions (sulfate, ammonium, nitrate) but contributing a significant proportion of total PM mass. The chemical complexity of PM makes it difficult to thoroughly characterize PM composition and to assess the contribution of individual components to health effects. Alternative indicators based on the mechanisms of PM toxicity, such as the oxidation potential (OP) of particles have been proposed to overcome this limitation.

Inhaled PM can initiate the production of reactive oxygen species (ROS) in target cells leading to oxidative stress[4]. This stress promotes an inflammatory response that should normally be transient but may be persistent in case of chronic exposure, and could induce some pathologies like asthma, chronic obstructive pulmonary disease and cardiovascular disease[5]. ROS production by PM is complex and involves both aerosol surface properties and chemical composition. In particular, metals and some organic compounds have been shown to contribute substantially to PM-induced ROS generation[6].

Generation of ROS by PM is responsible for the depletion of antioxidants present in the respiratory tract lining fluid (RTLF) covering the airways[7]. Furthermore, PM is able to generate ROS indirectly in cells by activation of different pathways. The measurement of the OP of particulate samples, by its integrative nature, could represent a new unifying metric to assess PM exposure in a more realistic way[8]. Different methods have been developed to measure the OP of ambient and engineered particles by measuring the consumption of antioxidants or the

oxidation of biomolecules[9-11]. Some of them have been implemented in monitoring sites to characterize PM exposure in epidemiological studies. However, contradictory results have been obtained so far. Several studies reported an association between OP and health outcomes[12-13] whereas others reported a lack of association[14]. A recent review[15] provides a thorough analysis of the different reasons that could explain such inconsistencies.

A wide range of cell-free assays are available to measure the inherent OP of ambient particles, but systematic cross-comparisons have only been performed on a limited number of assays. Hence, the predictive value of oxidative and inflammatory responses in target cells using a set of fully chemically characterized PM samples has never been assessed. As a follow-up of preliminary studies addressing this issue[6], the present study is performed on freshly sampled and chemically contrasted PM from traffic and domestic wood burning. We investigate here biological effects on two putative target cells: bronchial cells representing primary exposure targets and endothelial cells to mimic the cardiorespiratory outcome of $PM_{2.5}$. Then we apply the most predictive OP assay to characterize the temporal variability of chemically resolved PM.

The overall aim of this study is to determine whether the measurement of the intrinsic OP by four different cell-free assays can be predictive of the oxidative and proinflammatory responses induced in lung epithelial and endothelial cells exposed to $PM_{2.5}$ sampled at locations with contrasted combustion sources (traffic vs domestic wood burning). Next we investigated the temporal variability of both the OP and PM chemical components at these locations. We compared here $PM_{2.5}$ sampled at an urban traffic site with $PM_{2.5}$ sampled at a suburban site impacted by domestic wood burning.

Materials and Methods

PM collection and chemical characterization

Ambient $PM_{2.5}$ were sampled continuously (every 24h, from midnight to midnight UTC) at two distinct locations of the region of Paris using low volume Leckel sequential samplers (Model SEQ47/50, Sven Leckel Ingenieurbüro GmbH, Germany) running in parallel at 2.3m^3/h and equipped with 47-mm diameter Teflon (PTFE) and Quartz (TissuQuartz, Pallflex) filters. The first location ("Porte d'Auteuil") is situated near the ring road surrounding Paris and was chosen to sample $PM_{2.5}$ related to traffic (filter samples called "Traf"). Samples were collected in fall in order to avoid other sources of combustion such as domestic wood burning. The second location ("SIRTA"; Site Instrumental de Recherche par Télédétection Atmosphérique) is

located 20 km southwest of Paris center and can be considered as a suburban background station surrounded by cultivated areas, forests, and small towns. Sampling at this location was performed in winter when domestic heating is widely used yielding an aerosol enriched in particles from biomass burning (filter samples called "BB")[16]. For each site, samples were collected in three different periods: the first two consisting of batches of several (24-h sampled) filters that were merged in order to collect a sufficiently large mass of PM for chemical analysis and to realize both cell free assays and toxicological studies. The last sampling period consisted of daily sampling of $PM_{2.5}$ to study the temporal variability of the OP and link it to the day-to-day variability of the atmospheric concentration of individual PM chemical species (Table S1).

Chemical analyses of PM were performed on the Quartz filters running in parallel of the Teflon filters used for the different assays. They comprised: PM mass, major inorganic ions, carbonaceous aerosols: organic carbon (OC), elemental carbon (EC), carbohydrates including levoglucosan, a tracer of wood combustion, a total of 34 trace metals, a total of 16 Polyaromatic hydrocarbons (PAH) listed in SI. For each chemical analysis, standard operating procedures were performed as previously described[17-19].

The four PM batches (Traf1; Traf2; BB1; BB2; Table S1) obtained from the first two sampling periods were extracted from Teflon filters by immersion in methanol and strong sonication (Branson Digital Sonifier equipped with a cup-horn, 50%, 200 W) for 2 x 30 s. The volume of methanol in particle suspension was reduced by evaporation (Concentrator plus, Eppendorf, Montesson, France) at 30 °C. Final evaporation was performed under a constant flow of nitrogen. Extracted (dried) PM were stored at −20 °C until use. These PM samples were then suspended at the concentration of 2 mg/mL in 15 mM HEPES buffer. Particle suspensions were homogenized by sonication for 5 min at 200 W (5 s ON; 0.5 s OFF) (Branson Digital sonifier).

For the last sampling period (2-week continuous sampling; "daily sampling" in Table S1), OP assays were performed directly on filters. For this purpose, filters were cut in 1/32 portions, 3 of them being used for OP assay.

All chemicals for OP and biological assays were purchased from Sigma–Aldrich (Saint-Quentin Fallavier France) unless otherwise specified.

Intrinsic oxidative potential of PM

Dithiothreitol assay (DTT assay)

This assay quantitatively determines the oxidation of DTT by particles by measuring the consumption of reduced DTT[20]. In this assay, the transfer of electrons from DTT to oxygen generates DD-disulfide and superoxide radicals (O_2^{-}). The remaining non-oxidized DTT is then detected using the method described in[6]. The percentage of depletion is calculated as $\%PO^{DTT}$ depletion = 100 - ([DTT] sample/[DTT]control)*100).

Plasmid scission assay (Plasmid assay)

The plasmid scission assay quantify particle induced strand breaks in supercoiled φX174RF1 plasmid, caused by generation of free radicals[21]. Single strand breaks induce a relaxed circular form which migrates less rapidly during gel electrophoresis than the supercoiled plasmid. Detailed methodology is provided in[6]. The proportion of circularized DNA was calculated as a percentage of the supercoiled intact DNA. This percentage was then expressed for each condition relatively to the control.

Antioxidant depletion assay (AO assay)

This assay measures concentration variation of the antioxidants: ascorbic acid (AA), uric acid (UA) and glutathione (GSH), at physiological concentrations in presence of particle suspension[9, 22]. Particles from 10 to 100 µg/mL or 1/32 filters were incubated for 4 h at 37° C in a solution containing physiological concentrations (200 µM) of each AO in 0.9% NaCl at pH 7.4 with constant mixing. After incubation, the final AO concentrations in samples were quantified by reversed-phase HPLC (Shimadzu HPLC system interfaced with the LabSolution software) according to the method detailed in[6]. Percentage of depletion was calculated as: 100 - (AA or GSH concentration in the sample/ AA or GSH concentration in blank)*100 and GSSG production as (100 + (GSSG concentration in the sample/ GSSG concentration in blank)*100. For day-to-day samples results were expressed either per µg or per m^3 ($OP/m^3 = OP/\mu g * [PM]$).

CM-H_2DCF acellular assay

In this assay ROS produced by the particles convert the non-fluorescent CM-H_2DCF-DA ((5- (and-6) chloromethyl-2', 7'-dichlorodihydrofluorescein diacetate) probe (Fisher Scientific) into the fluorescent DCF (2', 7'-dichlorofluorescein). The detailed protocol is available in[6]. Briefly, CM-H_2DCFDA probe is first activated by an incubation with 10 mM of NaOH solution and further neutralized with 10X phosphate buffered saline without calcium and magnesium (PBS; Life Technologies, Thermo-Fisher Scientific). Particles from 10 to 100

µg/mL were incubated with 16.5 µM CM-H_2DCF in 96-well plate. Fluorescence generated by probe oxidation is read every hour for 4 h at 485 nm excitation and 520 nm emission, at 37°C with FlexStation 3 (Molecular Devices). Results were normalized to the control (probe solution without particles).

Cell culture and particle treatment

Human mucoepidermoid pulmonary carcinoma cell NCI-H292 (ATCC, Sigma), were grown as previously described[6]. PM were diluted in RPMI 1640 medium without phenol red and supplemented with 1% of penicillin-streptomycin and 1% of glutaMAX™ and NCI-H292 cells were exposed to concentrations of PM ranging from 1 to 10 µg/cm². For CM-H_2DCF assay, cells were grown in 96-well plates for fluorescence measurement at 4 and 24 h while for mRNA expression, cells were grown in 12-well plates during 24 h.

Human Pulmonary Artery Endothelial Cells (HPAEC) were isolated from the main branch of the pulmonary artery of a 23-year old male Caucasian donor. HPAEC were purchased from PromoCell® (France) and grown as described in[23]. HPAEC cells were exposed to concentrations from 1 to 10 µg/cm² of PM diluted in ECGM supplemented medium without phenol red. For mRNA expression, cells were grown in 12-well plates during 24 h while for CM-H_2DCF assay, cells were grown in 24-well plates for fluorescence measurement at 4 h.

CM-H_2DCFDA cellular assay

The probe used is the same as for the acellular assay, but without performing the activation step. CM-H_2DCFDA was dissolved in dimethyl sulfoxide (DMSO) at 2 mM and diluted (to 100 µM in RPMI 1640 medium for NCI-H292 and to 20 µM in HBSS for HPAEC). After washing (with PBS for NCI6H292 or HBSS for HPAEC), cells were loaded with the probe for 45 min with NCI6H292 or 20 min with HPAEC at 37° C in 96-well or 24-well plates. Cells were then washed twice with PBS or HBSS and exposed to particles for 4 h. Fluorescence was read at 485 nm excitation and 520 nm emission, at 37° C with FlexStation 3 (Molecular Devices) for NCI-H292 and FLUOstar Omega 2.10 plate reader with analyses performed using the MARS Data Analysis Software 2.30 R3 (BMG Labtech®) for HPAEC.

mRNA expression by RT-qPCR

TriReagent (TRI REAGENT®-RNA/DNA/Protein Isolation Reagent, Euromedex) was used for lyzing cells after 24 h of treatment. The manufacturer's recommendations RNA were used to perform RNA extraction and their quantification was done using Nanodrop 2000 (Thermo Scientific). 500 ng of oligo(dT) primers with M-MLV Reverse Transcriptase kit (Life Technologies, Thermo-Fisher Scientific) were added to 1 µg of total RNA to perform the

reverse transcription (RT) using a thermocycler (UNO II, Biometra). A Roche LC480 using LightCycler®480 SYBR Green 1 Master mix (Roche Diagnostics, Mannheim, Germany) was used to perform the quantitative PCR following the manufacturer's recommendations. The cycle threshold (CT) values were determined and normalized to HSC70 expression by the ΔΔCT method, using LightCycler®480 software v1.5. The conditions of PCR and the list of primers are detailed in the supplementary materials (Table S2).

Statistical analysis

Values are expressed as means ± standard error of the mean. Statistical analyses were conducted using either a one-way analysis of variance with Sidak's test for multiple comparisons or a two-way analysis of variance with Dunnett's test for multiple comparisons. For OP assays on daily samples, a Mann-Whitney test was performed. Bivariate correlations between OP and particle composition were quantified using non parametric Spearman correlation tests. GraphPad Prism v7.00 software was used to perform statistical analysis. The association between OP^{AO} and different particle concentrations was studied using multiple linear regression (MLR) analysis for both the BB and Traf sites according to the method described in SI.

Results and discussion

$PM_{2.5}$ from traffic and biomass burning exhibited distinct chemical signature

Both locations and periods of the year were selected to have compositionally distinct samples enriched for the specific chemical signature of the two main combustion sources (traffic, domestic wood burning). At the urban (Traffic, "Traf") site, $PM_{2.5}$ were sampled during Fall (when domestic heating is largely still off) and close to the Parisian ring road in order to have an aerosol enriched in diesel particles. At the suburban background (Biomass Burning, "BB") site situated at 20 km from Paris, particles were sampled in winter in order to have an aerosol enriched in combustion particles from domestic wood burning[16].

The average $PM_{2.5}$ mass concentrations were 15.01 ± 7.48 μg/m^3 and 26.4 ± 17.61 μg/m^3 at the Traf and BB sites respectively showing higher mass and higher daily variability at the BB site (Figure 1 and Figure S1). The high variability at the BB site was linked to 9 consecutive days with concentrations exceeding 25 μg/m^3 (03/14 to 03/21/2015) whereas this value was only exceeded two days at the Traf site (09/06 and 09/08/2013) (Figure S1). At the Traf site, the PM was dominated by carbonaceous compounds (OC + EC: 72.5%) whereas the BB site was characterized by a high inorganic ion content (NH_4^+ + NO_3^- + SO_4^{2-}= 73.85%) compared

to the carbonaceous content (OC + EC: 22.9%). The Traf site had an OC/EC ratio of 0.293 ± 0.091 whereas at the BB site this ratio was 4.55 ± 1.14, comparable to expected values for the respective sources of combustion particles (Figure S1)[16]. The Traf site had a higher metal content (683 ± 316 ng/m^3) compared to the BB site (114 ± 34 ng/m^3) both being dominated by Fe (Figure S2). At the Traf site, Cu, Mn, Mo, Sb, Sn, Fe were highly correlated ($r<0.915$, $p<0.0001$), likely a result of the contribution of non-tailpipe emissions such as brake/tire wear (Figure S3). Such correlations were not observed for the BB site (Figure S4). The Traf sample also had a higher PAH content (1.8 ± 0.515 ng/m^3 compared to 0.362 ± 0.116 ng/m^3 for BB site) with 2 PAHs (pyrene and Benzo(e)pyrene) representing 67% of the total PAHs at the Traf site (Figure S2). Correlations between PAHs were stronger at the BB site compared to the Traf site and most of the 17 analyzed PAHs were correlated to each other (Figure S5).

$PM_{2.5}$ from traffic and biomass burning sites exhibited distinct OP

Four different assays (AO depletion assay, DCF assay, DTT assay, plasmid scission assay) were used to compare the intrinsic OP of $PM_{2.5}$ sampled at both sites (Traf1; Traf2; BB1; BB2; Table S1). Two samples were collected at each site to avoid sampling bias. In contrast to many other published studies, these assays were performed using particle suspensions instead of water-soluble fractions for both cellular and cell-free assays to better account for oxidative stress related to particle uptake, water insoluble organic (e.g. PAH) and trace metals in intracellular ROS production. A dose-dependent strategy was chosen to better cover the range of OP according to the sites. In the AO depletion assay (Figure 2A and 2B), depletion of AA and GSH tended to increase as a function of dose. No modification of uric acid concentration was observed (data not shown), as was already described elsewhere for other $PM_{2.5}$ samples[6]. The two Traf samples (Traf1, Traf2) showed a 50% AA depletion from 25 µg/mL with nearly a total depletion at 100 µg/mL whereas for the samples at the BB site, the 50 % depletion was reached only at 100 µg/mL (Figure 2A). For all the concentrations, a clear difference was observed in AA depletion between Traf and BB samples. GSH depletion was less pronounced than AA depletion although samples showed a similar dose-dependent response. (Figure 2B). In the GSH assay, BB2 exhibited a higher response than BB1, closer to that of the Traf samples (Figure 2B). A corresponding difference between the two BB samples was also observed in GSSG production (Figure 2C). A high correlation was observed between GSH depletion and GSSG production ensuring that GSH depletion was the result of oxidation and not of a covalent binding to organic compounds ($r=0.965$). Moreover, the AA, GSH and GSSG data exhibited a

significant correlation between them (AA-GSH: 0.769, AA-GSSG: 0.664) (Table S3). The lower GSH depletion induced by PM compared to AA depletion and the correlation between GSH depletion and GSSG production confirmed previous results with other $PM_{2.5}$ samples[6]. With the DCF assay, BB samples never triggered an oxidation of the DCF probe whereas a similar dose-dependent effect was shown with the two Traf samples with a significant effect from 50 µg/mL (Figure 2D). The sensitivity of the DCF assay was previously observed with other Paris traffic samples[6, 23]. For the DTT assay, Traf samples exhibited a higher significant effect than BB samples at 10 µg/mL and DTT depletion was not increased at 100 µg/mL (Figure 2E) illustrating the non-linear DTT response to particle concentrations[24]. The DTT assay did not show significant correlation with OP^{AO} and OP^{DCF} assays (Table S3). For the semi-quantitative plasmid scission assay, a dose-dependent increase in DNA breaks was observed with a trend of a higher effect for Traf samples that is weak due to the high variability (Figure 2F). This assay provides the strongest correlations with other assays (Table S3). Correlations are weaker between other assays suggesting that each one, taken separately, could bring additional information on the PM chemical components involved in the assay. Therefore, several assays may have to be combined in order to provide a full picture of the ROS sources/mechanisms of generation. In a previous study, better correlations were observed between these assays although these correlations were derived from a higher number of PM samples[6]. Similarly, Calas et al., studying the seasonal variability of c.a.100 PM samples collected in the same city, observed a significant correlation between the different assays including DTT and AO (AA and GSH)[25].

Due to technical limitations, the availability of chemical data for these Traf and BB continuous samples was limited to trace metals. However, trace metal concentrations exhibited a strong correlation between continuous and daily samplings ($r=0.975$ and $r=0.98$ for the Traf and BB sites respectively) showing the consistency in particle composition over the whole sampling campaigns. Spearman correlation coefficients between trace metal concentrations and the different OP assays are shown in Table S4. Trace metals correlating positively with 5 or 6 OP assays were ranked according to decreasing sum correlation values: Mo>Mn>V>Ba>Zn>Fe>Sb>Cu>Sn. Among these, Cu, Mn, Mo, Sb, Sn and Fe were found to be co-correlated in the Traffic site and are markers of non-tailpipe emissions. This is consistent with the previously mentioned study, where Cu was the "unifying factor" among the OP assays that were used[25] as well as with data reported in a review on OP measurements across Italy[26].

$PM_{2.5}$ from traffic and domestic biomass burning sites produced distinct oxidative stress in both epithelial and endothelial cells

In addition to measurement of their inherent oxidative capacity, the same samples were evaluated for oxidative and pro-inflammatory responses on human lung epithelial and endothelial cells. Bronchial epithelial cells were selected as they are among the first cells encountered by inhaled particles. Endothelial cells are also directly influenced by inhaled particles as well as by particle-derived soluble compounds that translocate through the epithelial barrier.

The effect of $PM_{2.5}$ on the intracellular production of ROS was measured in epithelial and endothelial cells using the CM-H_2DCFDA probe. As shown in Figure 3 A and D, $PM_{2.5}$ induced an increase of the DCF fluorescence in both cell lines with increasing concentrations. Samples from the same site induced consistent effects and a clear difference was observed between Traf and BB samples in epithelial cells at the highest concentration (Figure 3A). By contrast no significant difference was seen between Traf and BB samples in exposed endothelial cells that otherwise showed a higher DCF oxidation (Figure 3D). No significant correlation was observed in DCF oxidation between the 2 cell types ($r=0.524$, $p>0.05$).

In order to determine whether this intracellular increase in ROS production was associated with an adaptive response to oxidative stress, heme-oxygenase-1 (HO-1) and superoxide dismutase-2 (SOD-2) expression were measured. The expression of these two anti-oxidant enzymes is driven by the activation of the transcription factor Nrf2 involved in the oxidative stress pathway. As shown Figure 3B and 3E, $PM_{2.5}$ induced a dose-dependent increase of the HO-1 expression in both cell lines, with the induction being higher in endothelial cells likely related to the higher ROS production. A clear difference in HO-1 expression is observed between Traf and BB samples at the highest tested concentrations in epithelial cells (Figure 3B) whereas for endothelial cells it was significant at 1 μg/cm² (Figure 3E). For SOD-2, no significant induction was shown in epithelial cells irrespective of the concentration and the type of $PM_{2.5}$ (Figure 3C). By contrast in endothelial cells, Traf 1 induced a significant upregulation of SOD-2 expression at 10 μg/cm² compared to BB2 $PM_{2.5}$ (Figure 3F). HO-1 and SOD-2 expression were significantly correlated in each cell types ($r=0.65$, $p<0.026$ in epithelial cells and $r=0.902$, $p<0.0001$ in endothelial cells). In epithelial cells, HO-1 and SOD-2 expression were significantly correlated to the intracellular DCF oxidation ($r=0.678$, $p<0.02$ for HO-1 and $r=0.769$, $p<0.005$ for SOD-2) whereas for endothelial cells a correlation with DCF was only observed with SOD-2 ($r=0.833$, $p<0.015$). Overall, it appears that endothelial cells exhibit a

more pronounced response than bronchial cells, which may imply a different sensitivity to oxidative stress. Correlations with trace metal content showed numerous significant correlations but the metals for which a significant correlation was observed for all 3 cellular endpoints and in both cell types were Bi, Ce, Cu, Mo, Pb, Sb, Se, Sn and V (Table S4).

$PM_{2.5}$ from traffic and domestic biomass burning sites induced pro-inflammatory response in epithelial and endothelial cells

IL-8 mRNA expression was used in both cell types to characterize the pro-inflammatory response. An increase of IL-8 mRNA expression was observed with exposure to both Traf and BB samples in both cell types (Figure S6). In endothelial cells a clear dose-response is observed for Traf and BB samples, with consistent results between samples of the same site. There was a significant difference between Traf and BB samples even at the lowest concentrations, BB samples being less reactive (Figure S6B). With epithelial cells, similar tendencies were observed but high within-site variability means that this data is not independently statistically significant (Figure S6A). However, a significant correlation is observed between the 2 cell types ($r=0.748$, $p<0.007$). The pro-inflammatory response is often considered to be related to oxidative stress, which is supported in this experiment by the strong correlation between IL-8 expression and HO-1 and SOD-2 expression in each cell type ($r=0.573$, $p<0.056$ (HO-1), $r=0.916$, $p<0.0001$ (SOD-2) for epithelial cells, and $r=0.846$, $p<0.001$ (HO-1) and $r=0.881$, $p<0.0001$ (SOD-2) for endothelial cells).

Lung antioxidant depletion assay is the most predictive OP assay of cell responses

In order to determine which OP assays were better predictors of oxidative cell responses, correlation studies were performed (Table S5). The $OP^{plasmid}$ assay provides the best correlation with other cell-free and cell assays but due to its semi-quantitative and time-consuming nature, it was not considered for further experiments. OP^{AA} and OP^{DCF} also give the most significant correlations for the 2 cell types. The OP^{AO} includes the simultaneous detection of depletion or oxidation of two antioxidants, and by combining these measurements it covers several possible cellular responses. Especially noteworthy is the high degree of correlation between OP^{AO} endpoints and HO-1 expression in both cell types.

Taking into consideration the correlation between OP^{AO} and cellular responses as well as the opportunity to measure different anti-oxidants and the formation of an oxidation product

in the same assay, we focused on the OP^{AO} assay to realize a daily characterization of OP of $PM_{2.5}$ sampled at the 2 sites over 3 weeks (Table S1). Furthermore, OP^{AO} assays could be validated using filters instead of particle suspensions whereas this is not possible for the plasmid assay (Figure S7).

Daily analysis of OP^{AO} always revealed a higher OP for $PM_{2.5}$ from traffic site compared to biomass burning site

OP^{AO} was measured on $PM_{2.5}$ sampled for 24h during n=19 and n=22 consecutive days at the Traf and BB sites respectively. Compared to blank filters, all daily samples exhibited, a clear temporal variability with a depletion of AA (Figure 4) and GSH (Figure S8) and a production of GSSG (Figure S9). For both sites, GSH depletion correlated well to GSSG production (r=0.945 for Traf site and r=0.978 for BB site, p<0.0001). Independently of the site, the depletion was systematically larger for AA than for GSH (Figure 4, and Figure S8 respectively) but a significant correlation was observed between OP^{AA} and OP^{GSH} (r=0.784, p<0.0001 for OP/m^3 and r=0.914 for OP/µg, p<0.0001). OP^{AA} when expressed per m^3, showed a temporal variability directly related to ambient $PM_{2.5}$ concentrations. OP^{AA} measurements from Traf site samples were significantly higher (1.39±0.25) than OP^{AA} from BB site samples (0.910±0.252) with a ratio Traf/BB of 1.52 (p<0.001, Figure 4A, B, C). When OP^{AA} was expressed per µg of PM, a temporal variability was again observed reflecting the contribution of PM components to OP, and OP^{AA} measurements from Traf site samples were significantly higher (0.098±0.036) than OP^{AA} from BB site samples (0.044±0.021) with a ratio Traf/BB of 2.22 (p<0.0001, Figure 4D, E, F). At the BB site, the OP^{AA}/µg was particularly low during a period when $PM_{2.5}$ mass was high due to the increase of secondary pollutants such as ions and organics in PM, which are considered not to contribute significantly to OP (Figure 1).

No correlation was observed between OP^{AA}/m^3 and OP^{AA}/µg suggesting that OP was not directly proportional to ambient PM concentrations. The same conclusions were obtained with OP^{GSH} and OP^{GSSH} with significant differences between the two sites considering results expressed per m^3 or µg but with less magnitude (Figure S8, S9). Altogether these data clearly underline the major role of PM composition in OP.

To further explore site-to-site differences in OP, we examined multivariable linear regression (MLR) models in order to characterize the relationships between PM chemical composition and OP^{AA}. The MLR analyses were performed using volume based data and PAH, trace metals or ion descriptor sets, separately or together. We selected descriptors that contributed more than 0.9 in terms of R^2 when possible at Traf and BB sites (Table 1).

For the Traf site, OP^{AA} is very well explained by a panel of 8 trace metal descriptors (R^2=0.856) with Ti and Mo being the strongest contributors and well explained by PAH (R^2_{adj}=0.646) but not by ions (R^2_{adj}=0.075) (Table 1 and figure S10). Considering all components measured (PAH, trace metals, ions) including OC and EC, the combination of descriptors BaA, Al, Pb, As, BbF, NO_3, Sr and Ti improves the model (R^2_{adj}=0.923). For the BB site, OP^{AA} is similarly very well explained by trace metals (R^2_{adj}=0.907, 13 descriptors) and well explained by PAH (R^2_{adj}=0.559, 1 descriptor). In addition, OP^{AA} is well explained by ions (R^2_{adj}=0.857, 4 descriptors). When all components are considered (including OC and EC), 4 descriptors (Cu, K, SO_4^{2-} and Mo) were sufficient to obtain a model with R^2_{adj}=0.906. Next important descriptor to improve the R^2_{adj} is OC from 0.906 to 0.920. Levoglucosan data is available for this site and its addition in the model increases the correlation to R^2_{adj}=0.914 whereas substituting it for K decreases the correlation to R^2_{adj}=0.873. The strong contribution to the regression by tracers of biomass burning supports the contribution of this source to the overall OP^{AA} of the BB samples. The similar values of R^2_{adj} and R^2_{LOO} obtained confirm the stability of the regression models for both Traf and BB sites.

The same analysis was performed for OP^{GSH} (table S6 and figure S10). It provides consistent quality of regression models but involves different descriptors suggesting that these two OP do not react with the same components of the sample. Like OP^{AA}, OP^{GSH} is very well explained by a panel of several metal descriptors (R^2_{adj}=0.825 for Traf and 0.932 for BB sites) and that regression models are improved by combining different types of descriptors (R^2_{adj}=0.913 for Traf and 0,919 for BB sites). In summary, adequate explanation of the measured OP requires a site-specific regression model which accounts for differences in chemical components arising from different emission sources. Similar conclusions were recently drawn by Weichenthal, concerning within-city variations of $PM_{2.5}$ OP^{AO} in Toronto[27].

In this study we provided evidence that OP measurement is predictive of cellular oxidative and pro-inflammatory responses strengthening the idea that OP of PM could be used as a biologically-relevant exposure metric for studies of air pollution and health. Modelling approaches using source apportionment are currently being developed to determine the contribution of natural and anthropogenic sources to PM-OP and to estimate OP over a large spatio-temporal scale[28-29]. Whether OP predicts health effects better than currently regulated PM characteristics, including mass and composition is not yet fully supported in epidemiological studies exhibiting either the absence or positive association[12-14, 30-31].

Contradictory results obtained in such studies could result from the present lack of standardized protocols for particle extraction and OP assays[25].

Associated content

Supporting Information

Supporting information consists of details of methodology, 11 figures, and 6 tables.

Conflict of interest: The authors declare that they have no conflict of interest.

Acknowledgment and grant information: This work was supported by the French Environment and Energy Management Agency (ADEME: convention n° 1262C0037) in the context of the call for research proposals of the national research program for environmental and occupational health (PNREST) 2012 of ANSES (French Agency for Food, Environmental and Occupational Health & Safety) under grant n° 2012-2-013, project "POTOX". We also acknowledge the platform "FlexStation" and the platform "Bioprofiler" for HPLC analysis of the facility "Métabolisme" (Univ de Paris, Unité de Biologie Fonctionnelle et Adaptative (BFA) UMR 8251 CNRS, F-75205, Paris, France), for spectrophotometric analysis. We thank Léa Baudas that contributes to OP measurements during her 2 month internship and Oliver Brookes for English proofreading and editing.

References

(1) Landrigan, P. J., Fuller, R., Acosta, N. J. R., Adeyi, O., Arnold, R., Basu, N. N., Baldé, A. B., Bertollini, R., Bose-O'Reilly, S., Boufford, J. I., Breysse, P. .N., Chiles, T., Mahidol, C., Coll-Seck, A. M., Cropper, M. L., Fobil, J., Fuster, V., Greenstone, M., Haines, A., Hanrahan, D., Hunter, D., Khare, M., Krupnick, A., Lanphear, B., Lohani, B., Martin, K., Mathiasen, K. V., McTeer, M. A., Murray, C. J. L., Ndahimananjara, J. D., Perera, F,. Potočnik, J., Preker, A. S., Ramesh, J., Rockström, J., Salinas, C., Samson, L. D., Sandilya, K., Sly, P. D., Smith, K. R., Steiner, A., Stewart, R. B., Suk, W. A., van Schayck, O. C. P., Yadama, G. N., Yumkella, K., Zhong, M. The Lancet Commission on pollution and health. *Lancet*. **2018,** 391(10119):462-512; DOI 10.1016/S0140-6736(17)32345-0.

(2) Mukherjee, A., Agrawal, M. A. Global Perspective of Fine Particulate Matter Pollution and Its Health Effects. *Rev. Environ. Contam. Toxicol*. **2018**, 244:5-51.

(3) Review of evidence on health aspects of air pollution – REVIHAAP Project: Technical Report. WHO Regional Office for Europe. http://www.euro.who.int/en/health-topics/environment-and-health/air-quality/publications/2013/review-of-evidence-on-health-aspects-of-air-pollution-revihaap-project-final-technical-report

(4) Nel, A. Air-pollution related-illness: effects of particles. *Science,* **200,**. 423, 804-806; DOI 10.1126/science.1108752

(5) Li, R., Zhou, R., Zhang, J. Function of PM2.5 in the pathogenesis of lung cancer and chronic airway inflammatory diseases. *Oncol. Lett*. **2018,** 15(5):7506-7514; DOI 10.3892/ol.2018.8355.

(6) Crobeddu, B., Aragao-Santiago, L., Bui, L. C., Boland, S., Baeza Squiban A. Oxidative potential of particulate matter 2.5 as predictive indicator of cellular stress. *Environ. Pollut.* **2017**, 230:125-133; DOI 10.1016/j.envpol.2017.06.051.

(7) Kelly, F. J., Fussell, J. C. Linking ambient particulate matter pollution effects with oxidative biology and immune responses. *Ann. N. Y. Acad. Sci*. **2015**, 1340:84-94; DOI 10.1111/nyas.12720.

(8) Janssen, N. A., Strak, M., Yang, A., Hellack, B., Kelly, F. J., Kuhlbusch, T. A., Harrison, R. M., Brunekreef, B., Cassee, F. R., Steenhof, M., Hoek, G. Associations between three specific a-cellular measures of the oxidative potential of particulate matter and markers of acute airway and nasal inflammation in healthy volunteers. *Occup. Environ. Med*. **2015**, 72(1):49-56; DOI: 10.1136/oemed-2014-102303

(9) Ayres, J. G.; Borm, P.; Cassee, F. R.; Castranova, V.; Donaldson, K.; Ghio, A.; Harrison, R. M.; Hider, R.; Kelly, F.; Kooter, I. M.; Marano, F.; Maynard, R. L.; Mudway, I.; Nel, A.; Sioutas, C.; Smith, S.; Baeza-Squiban, A.; Cho, A.; Dugganv S.; Froines, J.. Evaluating the toxicity of airborne particulate matter and nanoparticles by measuring oxidative stress potential--a workshop report and consensus statement. *Inhal Toxicol*. **2008**, 20(1):75-99; DOI 10.1080/08958370701665517

(10) Hellack, B.; Nickel, C.; Albrecht, C.; Kuhlbusch, T. A. J.; Boland, S.; Baeza-Squiban, A.; Wohlleben, W.; Schins, R. P. F. Analytical methods to assess the oxidative potential of nanoparticles: a review. *Environ Sci Nano*. **2017**, 4, 1920-1934; DOI 10.1039/C7EN00346C

(11) Bates, J. T., Fang, T., Verma, V., Zeng, L., Weber, R. J., Tolbert, P. E., Abrams, J. Y., Sarnat, S. E., Klein, M., Mulholland, J. A., Russell, A. G. Review of Acellular Assays of Ambient Particulate Matter Oxidative Potential: Methods and Relationships with Composition, Sources, and Health Effects. *Environ Sci Technol*. **2019**, 53(8):4003-4019; DOI 10.1021/acs.est.8b03430

(12) Maikawa, C. L.; Weichenthal, S.; Wheeler, A. J.; Dobbin, N. A.; Smargiassi, A.; Evans, G; Liu, L.; Goldberg, M. S.; Pollitt, K. J. Particulate Oxidative Burden as a Predictor of Exhaled Nitric Oxide in Children with Asthma. *Environ. Health Perspect*. **2016**, 124(10):1616-1622; DOI 10.1289/EHP175

(13) Weichenthal, S.A. ; Lavigne, E. ; Evans, G.J. ; Godri Pollitt, K.J. ; Burnett, R.T. PM2.5 and Emergency Room Visits for Respiratory Illness: Effect Modification by Oxidative Potential. *Am. J. Respir. Crit. Care Med*. **2016**, 194(5):577-86; DOI: 10.1164/rccm.201512-2434OC

(14) Fang, T., Verma, V., Bates, J. T., Abrams, J., Klein, M., Strickland, M. J., Sarnat, S. E., Chang, H. H., Mulholland, J. A., Tolbert, P. E., Russell, A. G., Weber R. J. Oxidative potential of ambient water-soluble PM2.5 in the southeastern United States: contrasts in sources and health associations between ascorbic acid (AA) and dithiothreitol (DTT) assays, *Atmos. Chem. Phys*. **2016**, 16, 3865-3879. DOI 10.5194/acp-16-3865-2016

(15) Øvrevik, J. Oxidative Potential Versus Biological Effects: A Review on the Relevance of Cell-Free/Abiotic Assays as Predictors of Toxicity from Airborne Particulate Matter. *Int. J. Mol. Sci*. **2019**, 20(19). pii: E4772. DOI: 10.3390/ijms20194772.

(16) Petit, J. E., Favez, O., Sciare, J., Crenn, V., Sarda-Estève, R., Bonnaire, N., Dupont, J. C., Močnik, G., Haeffelin, M., Leoz-Garziandia, E. Two years of near real-time chemical composition of submicron aerosols in the region of Paris using an Aerosol Chemical

497 Speciation Monitor (ACSM) and a multi-wavelength Aethalometer. **2015**, *Atmos. Chem.*
498 *Phys.*, 15, 2985-3005, DOI 10.5194/acp-15-2985-2015
499 (17) Sciare, J., d'Argouges, O., Sarda-Estève, R., Gaimoz, C., Dolgorouky, C., Bonnaire, N.,
500 Favez, O., Bonsang, B., Gros, V. Large contribution of water-insoluble secondary
501 organic aerosols in the region of Paris (France) during wintertime. *J. Geophys. Res*. **2011,**
502 116, D22203; DOI 10.1029/2011JD015756.
503 (18) Panteliadis, P., Hafkenscheid, T., Cary, B., Diapouli, E., Fischer, A., Favez, O.,
504 Quincey, P., Viana, M., Hitzenberger, R., Vecchi, R., Maggos, T., Sciare, J., Jaffrezo, J.
505 L., John, A., Schwarz, J., Giannoni, M., Novak, J., Karanasiou, A., Fermo, P., Maenhaut,
506 W. ECOC comparison exercise with identical thermal protocols after temperature offsets
507 correction. Instrument diagnostics by in-depth evaluation of operational parameters.
508 **2015***, Atmos. Meas. Tech.*, 8, 779-792; DOI 10.5194/amt-8-779-2015
509 (19) Yttri, K. E., Schnelle-Kreiss, J., Maenhaut, W., Alves, C., Bossi, R., Bjerke, A., Claeys,
510 M., Dye, C., Evtyugina, M., García-Gacio, D., Gülcin, A., Hillamo, R., Hoffer, A.,
511 Hyder, M., Iinuma, Y., Jaffrezo, J.-L., Kasper-Giebl, A., Kiss, G., López-Mahia, P. L.,
512 Pio, C., Piot, C., Ramirez-Santa-Cruz, C., Sciare, J., Teinilä, K., Vermeylen, R., Vicente,
513 A., Zimmermann, R. An intercomparison study of analytical methods used for
514 quantification of levoglucosan in ambient aerosol filter samples. *Atmos. Meas. Tech*.
515 **2015**, 8, 125-147; DOI 10.5194/amt-8-125-2015
516 (20) Cho, A. K., Sioutas, C., Miguel, A. H., Kumagai, Y., Schmitz, D. A., Singh, M.,
517 Eiguren-Fernandez, A., Froines, J. R. Redox activity of airborne particulate matter at
518 different sites in the Los Angeles Basin. *Environ. Res*. **2005**, 99, 40-47.
519 (21) Donaldson, K., Brown, D. M., Mitchell, C., Dineva, M., Beswick, P. H., Gilmour, P.,
520 MacNee, W. Free radical activity of PM10: iron-mediated generation of hydroxyl
521 radicals. *Environ. Health Perspect*. **1997** 105 Suppl 5:1285-1289.
522 (22) Mudway, I. S., Stenfors, N., Blomberg, A., Helleday, R., Dunster, C., Marklund, S. L.,
523 Frew, A. J., Sandström, T., Kelly, F. J. Differences in basal airway antioxidant
524 concentrations are not predictive of individual responsiveness to ozone: a comparison of
525 healthy and mild asthmatic subjects. *Free Radic. Biol. Med*. **2001**, 31(8):962-74; DOI
526 10.1016/S0891-5849(01)00671-2
527 (23) Deweirdt, J., Quignard, J. F., Crobeddu, B., Baeza-Squiban, A., Sciare, J., Courtois, A.,
528 Lacomme, S., Gontier, E., Muller, B., Savineau, J. P., Marthan, R., Guibert, C.,
529 Baudrimont, I. Involvement of oxidative stress and calcium signaling in airborne

particulate matter - induced damages in human pulmonary artery endothelial cells. *Toxicol. In Vitro*. **2017**, 45(Pt 3):340-350; DOI 10.1016/j.tiv.2017.07.001.

(24) Charrier, J. G., Mcfall, A. S., Vu, K. K., Baroi, J., Olea, C., Hasson, A. and Anastasio, C. A bias in the "mass-normalized" DTT response – An effect of non-linear concentration-response curves for copper and manganese. *Atmos. Environ*. **2016,** 144, 325–334.

(25) Calas, A., Uzu, G., Martins, J. M. F., Voisin, D., Spadini, L., Lacroix, T., Jaffrezo, J. L. The importance of simulated lung fluid (SLF) extractions for a more relevant evaluation of the oxidative potential of particulate matter. *Sci Rep*. **2017,** 7(1):11617; DOI 10.1038/s41598-017-11979-3.

(26) Pietrogrande, M. C., Russo, M., Zagatti, E. Review of PM Oxidative Potential Measured with Acellular Assays in Urban and Rural Sites across Italy. *Atmosphere*. **2019**, 10(10), 626, DOI 10.3390/atmos10100626

(27) Weichenthal, S., Shekarrizfard, M., Traub, A., Kulka, R., Al-Rijleh, K.., Anowar, S., Evans, G., Hatzopoulou, M. Within-City Spatial Variations in Multiple Measures of PM2.5 Oxidative Potential in Toronto, Canada. *Environ Sci Technol*. **2019**, 53(5):2799-2810. DOI 10.1021/acs.est.8b05543.

(28) Bates, J. T., Weber, R. J., Verma, V., Fang, T., Ivey, C., Liu, C., Sarnat, S. E., Chang, H. H, Mulholland, J. A., Russell, A. G. Source impact modeling of spatiotemporal trends in PM2.5 oxidative potential across the eastern United States. *Atmos. Environ.* **2018**, 193, 158-167; DOI 10.1016/j.atmosenv.2018.08.055

(29) Weber, S., Uzu, G., Calas, A., Chevrier, F., Besombes, J. L., Charron, A., Salameh, D., Ježek, I., Močnik, G., Jaffrezo, J. L. An apportionment method for the oxidative potential of atmospheric particulate matter sources: application to a one-year study in Chamonix, France. *Atmos. Chem. Phys*. **2018,** 18, 9617–9629, DOI 10.5194/acp-18-9617-2018

(30) Atkinson, R. W.; Mills, I. C.; Walton, H. A.; Anderson, H. R. Fine particle components and health--a systematic review and meta-analysis of epidemiological time series studies of daily mortality and hospital admissions. *J. Expo. Sci. Environ. Epidemiol*. **2015,** 25(2):208-14; DOI 10.1038/jes.2014.63

(31) Zhang, X., Staimer, N., Tjoa, T., Gillen, D.L., Schauer, J.J., Shafer, M.M., Hasheminassab, S., Pakbin, P., Longhurst, J., Sioutas, C., Delfino, R.J. Associations between microvascular function and short-term exposure to traffic-related air pollution and particulate matter oxidative potential. *Environ. Health*. **2016**, 15(1):81; DOI 10.1186/s12940-016-0157-5

564

565 Table 1: **Results of multivariate linear regression analysis between PM chemical**
566 **composition and OP^{AA}** with R^2_{adj}, R^2_{LOO} indicated

	Traffic (n=19)	**Biomass Burning (n=22)**
PAH	BaA, CHR, BbF, BeP R^2_{adj} = 0.646, R^2_{LOO} = 0.647 (± 0.019)	BeP R^2_{adj} = 0.559, R^2_{LOO} = 0.559 (± 0.039)
Trace metals	Ti, Mo, Pb, As, Co, Al, Ba, Sb R^2_{adj} = 0.856, R^2_{LOO} = 0.856 (± 0.021)	Cu, Mo, Hg, Zn, Rb, As, Sr, Ti, Ce, Li, V, Al, Se R^2_{adj} = 0.907, R^2_{LOO} = 0.908 (± 0.017)
Ions	Na R^2_{adj} = 0.075, R^2_{LOO} = 0.074 (± 0.029)	K, Cl, Mg^{2+}, Na, Ca^{2+} R^2_{adj} = 0.857, R^2_{LOO} = 0.857 (± 0.021)
All components	BaA, Al, Pb, As, BbF, NO_3^-, Sr, Ti R^2_{adj} = 0.923, R^2_{LOO} = 0.893 (± 0.029)	Cu, K, SO_4^{2-}, Mo R^2_{adj} = 0.906, R^2_{LOO} = 0.842 (± 0.017)

567 benzo(a)anthracene (BaA), chrysene (CHR), benzo(e)pyrene (BeP), benzo(b)fluoranthene (BbF)

568

569

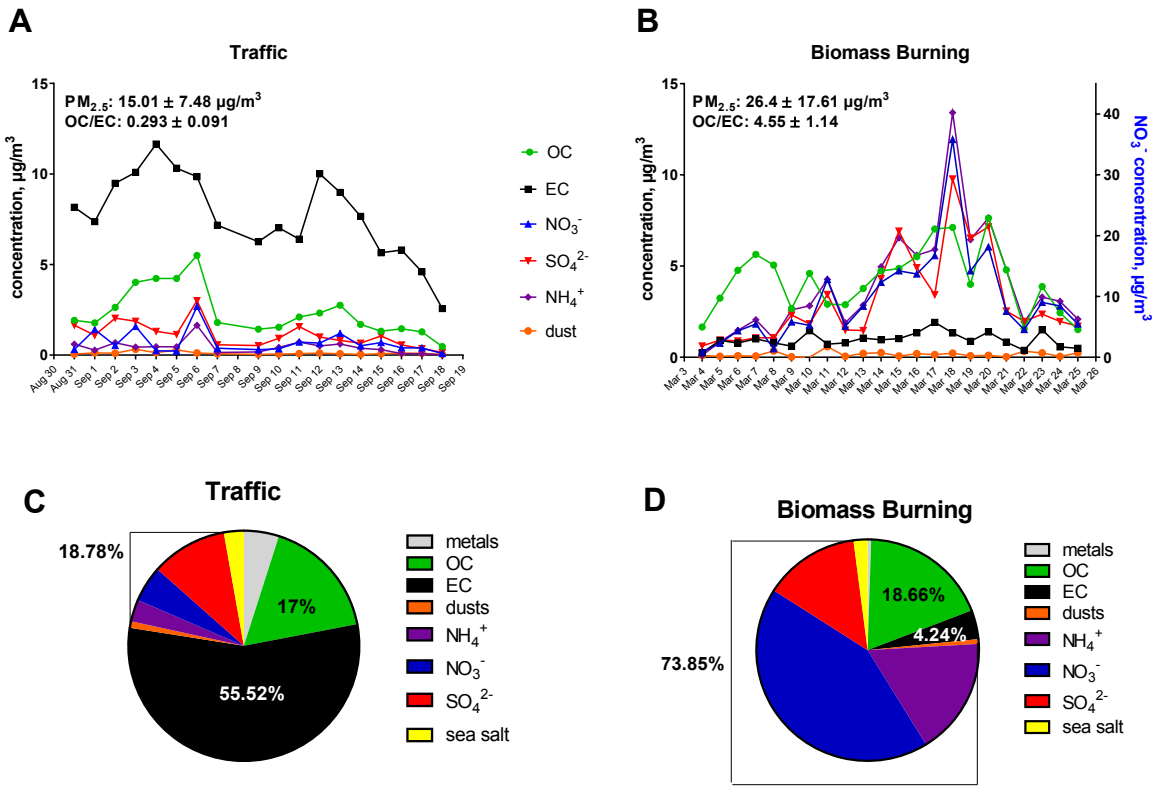

570

571 **Figure 1: Main $PM_{2.5}$ chemical components at the Traffic (A-C) and Biomass Burning (B-**
572 **D) sites.** Daily concentrations (µg/m^3) of carbonaceous (organic carbon (OC) and elemental
573 (EC)) compounds, inorganic ions (NH_4^+, NO_3^-, SO_4^{2-}) and dusts for the Traffic (A) and Biomass
574 Burning (B) sites. Mass distribution of the main chemical components in $PM_{2.5}$ from the Traffic
575 (C) and Biomass burning (D) sites. The numbers on the left side of the pie chart represent the
576 proportion of inorganic ion content ($NH_4^+ + NO_3^- + SO_4^{2-}$).

577

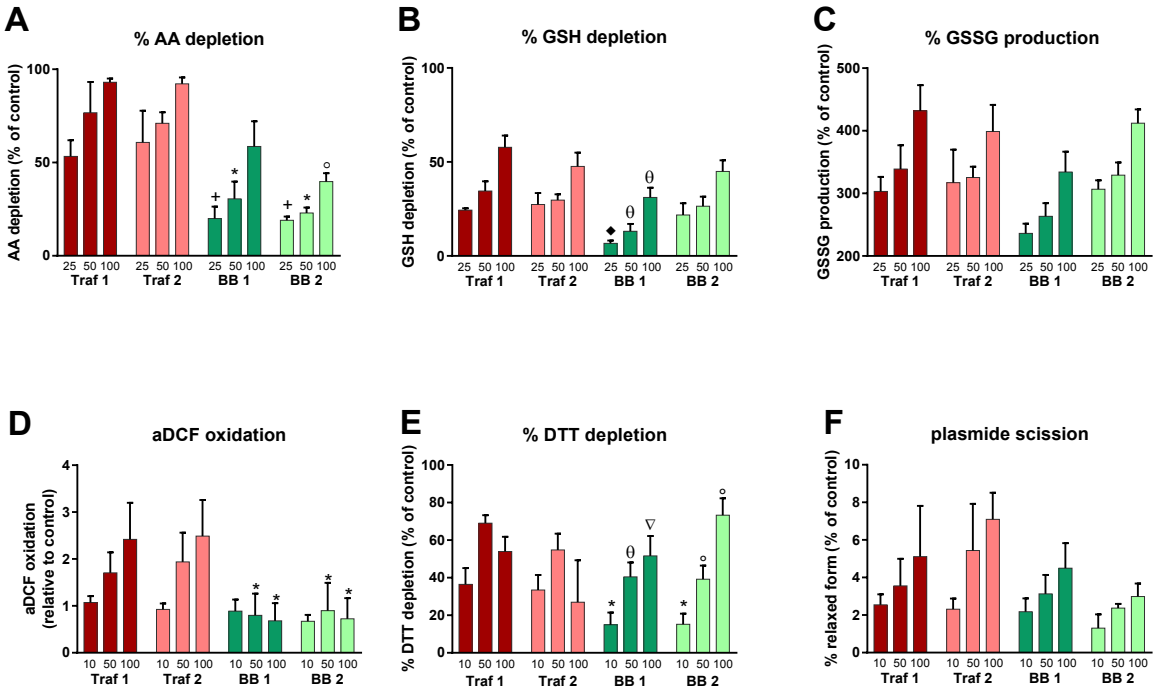

Figure 2: **Intrinsic oxidative capacity of $PM_{2.5}$ sampled at Traffic and Biomass Burning sites characterized through different oxidative potential assays**. Measurement of A) acid ascorbic (AA) depletion B) reduced glutathione (GSH) depletion C) oxidized glutathione (GSSG) production in a simplified synthetic respiratory tract lining fluid after a 4 h incubation at 37°C in presence of 25 to 100 µg/mL of $PM_{2.5}$ (2 different traffic sites (Traf 1 and Traf2) and biomass burning sites (BB 1 and BB 2). Results are expressed as the percentage of initial AO concentrations (200 µM) in the sRTLF and data are represented as mean ± SEM of 2 independent experiments with 3 replicates. D) The fluorescence of the oxidized CM-DCF was measured after 2 h of incubation at 37°C in presence of 10 to 100 µg/mL of $PM_{2.5}$. Results were normalized to the control and data are represented as mean ± SEM of 3 independent experiments of 4 replicates. Measurement of reduced DTT remaining after incubation in the presence of 10 to 100 µg/mL of $PM_{2.5}$ during 1 h at 37°C. Results are expressed as percentage of reduced DTT depletion relatively to control and data are represented as mean ± SEM of 3 independent experiments with 3 replicates. F) Quantification of relaxed circular form of DNA produced after 4 h of incubation at 37°C in the presence of H_2O_2 or 10 to 100 µg/mL of $PM_{2.5}$. Results are expressed as the percentage of relaxed circular form relative to the supercoiled intact DNA and data are represented as mean ± SEM of 3 independent experiments with 3 replicates. * $p<0.05$ between Traf and BB samples at the same dose, + $p<0.05$ between Traf 2 and BB samples at the same dose, ° $p<0.05$ between Traf and BB2 sample at the same dose, Θ $p<0.05$ between

598 Traf 1 and BB1 sample at the same dose, ∇ $p<0.05$ between Traf 2 and BB1 sample at the same
599 dose, ♦ $p<0.05$ between Traf and BB1 sample at the same dose.

600

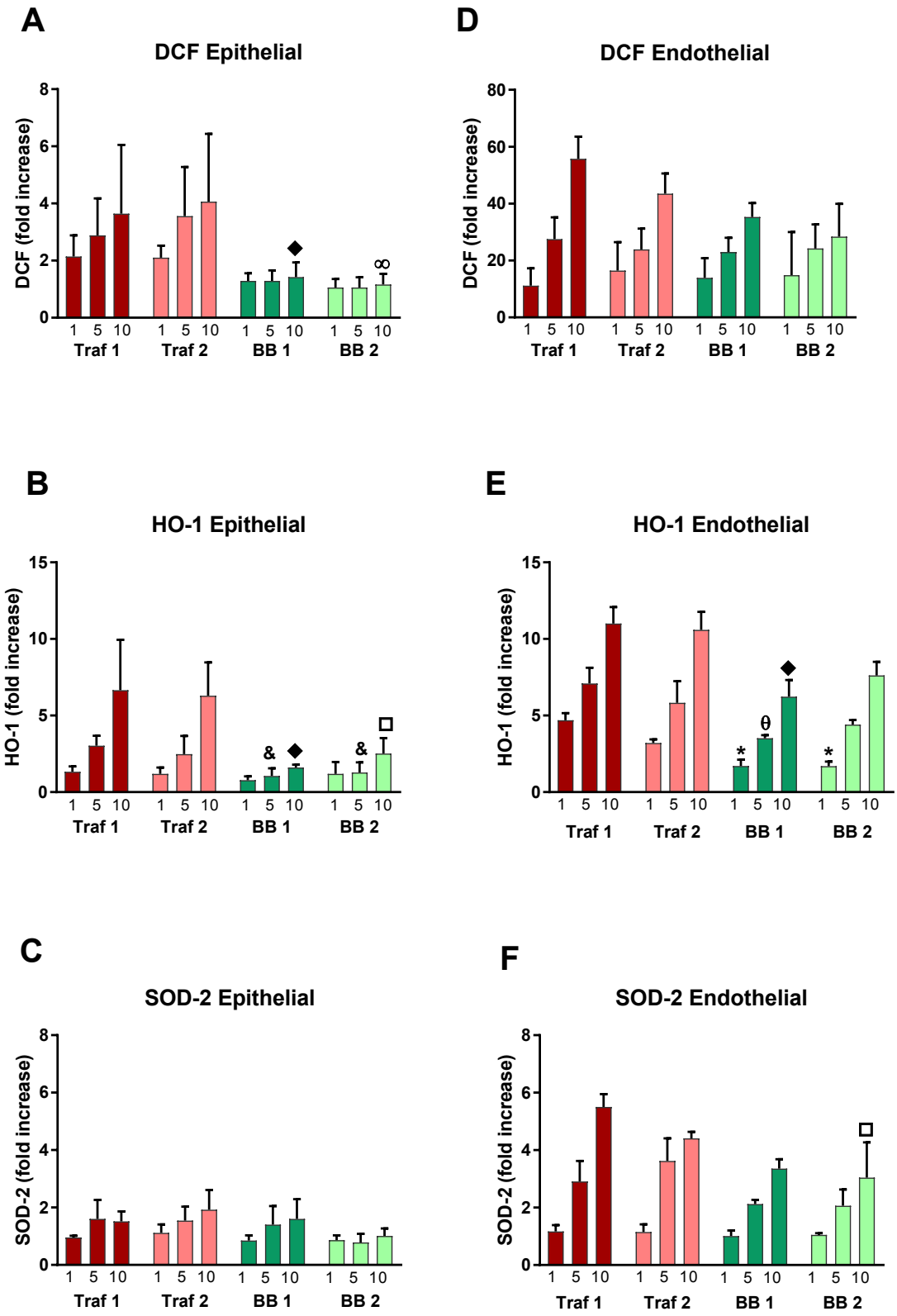

Figure 3: **ROS production and antioxidant responses in bronchial epithelial (A, B, C) and pulmonary endothelial (D, E, F) cells exposed to $PM_{2.5}$ sampled at Traf and BB sites**. Measurement of A-D) DCF fluorescence to assess the intracellular ROS production in cells exposed to $PM_{2.5}$ for 4 h, B-E) HO-1 (Heme-oxygenase-1) mRNA expression in cells exposed

606 to 1 to 10 μg/cm² of $PM_{2.5}$ for 24 h, C-F) SOD-2 (superoxide dismutase-2) mRNA expression
607 in cells exposed to 1 to 10 μg/cm² of $PM_{2.5}$ for 24 h. Results are normalized to control and data
608 are presented as mean ± SEM of 2 independent experiments with 3 replicates. * $p<0.05$ between
609 Traf and BB samples at the same dose, ∞ $p<0.05$ between Traf 2 and BB2 sample at the same
610 dose, Θ $p<0.05$ between Traf 1 and BB1 sample at the same dose, ♦ $p<0.05$ between Traf and
611 BB1 sample at the same dose, & $p<0.05$ between Traf 1 and BB samples at the same dose, □
612 $p<0.05$ between Traf 1 and BB2 sample at the same dose.

613

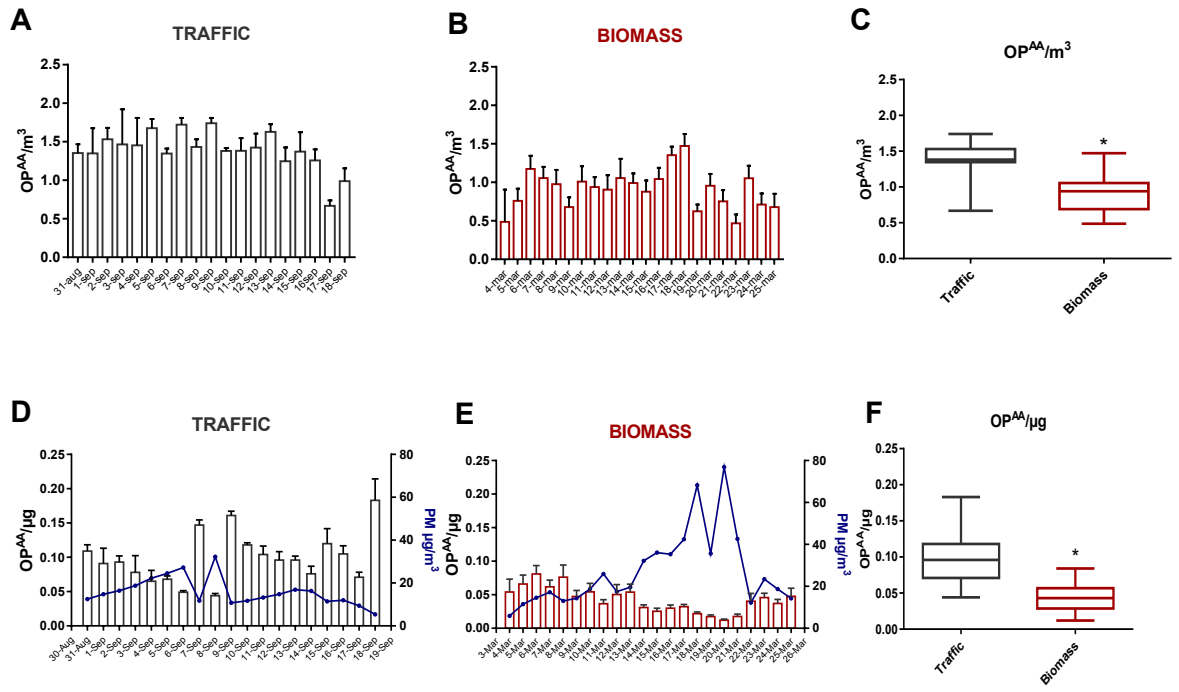

614

615 Figure 4: **Ascorbic acid depletion (OP^{AA}) of daily PM samples collected at the Traffic sites**
616 **Traffic, A and D) or at the Biomass Burning sites (Biomass, B and E).** Results are expressed
617 per m^3 (A and B) or per µg (D and E). In addition to OP^{AA}, $PM_{2.5}$ concentrations expressed as
618 $\mu g/m^3$ are shown on D and E (blue curve). C and F box plots representation showing the median,
619 25th and 75th percentile for the OP^{AA} in each site expressed per m^3 (C) or per/µg (F). Mann
620 Whitney *$p<0.0001$

621